

Performance Analysis of Integrated GPS/GLONASS Carrier Phase-Based Positioning

Liwen Dai
Shaowei Han
Chris Rizos

*School of Geomatic Engineering
The University of New South Wales
Sydney NSW 2052
Australia*

Tel: 61 2 9385 4206
Fax: 61 2 9313 7493
Email:liwen@unsw.edu.au

ABSTRACT

Due to the different signal frequencies for the GLONASS satellites, the commonly used double-differencing procedure for carrier phase data processing cannot be implemented in its straightforward form, as in the case of GPS. In this paper a novel data processing strategy for integrated GPS/GLONASS positioning is proposed, involving a three-step procedure. The first step is pseudo-range-based positioning, using double-differenced (DD) GPS pseudo-range and single-differenced (SD) GLONASS pseudo-range measurements, to derive the initial position and receiver clock bias. The second step is to form DD measurements (expressed in cycles) in order to estimate the ambiguities, using the receiver clock bias as estimated in the previous step. The third step is to form DD measurements (expressed in metric units) with the unknown SD integer ambiguity for the GLONASS reference satellite as the only parameter (which is constant until a cycle slip occurs for this satellite). A real-time stochastic model estimated by residual series over previous epochs is proposed for integrated GPS/GLONASS carrier phase and pseudo-range data processing. Other associated issues, such as cycle slip detection, validation criteria and adaptive procedure(s) for ambiguity resolution, will also be discussed. The performance of this data processing strategy will be demonstrated through case study examples of rapid static positioning and kinematic positioning. Based on four experiments carried out to date, the results indicate that rapid static positioning requires 1 minute of single frequency GPS/GLONASS data for 100% positioning success rate. The single epoch positioning solution for kinematic positioning can achieve 94.6% success rate over short baselines (<6km).

KEY WORDS GPS/ GLONASS, Stochastic Model, Functional Model, Ambiguity Resolution

BIOGRAPHY

Liwen Dai received a B.Sc. and M.Sc. in Geodesy in 1995 and 1998 respectively, from the Wuhan Technical University of Surveying and Mapping (WTUSM), P.R. China. He is currently a Ph.D. student at The University of New South Wales (UNSW), Australia.

Shaowei Han is Principal Scientist in Magellan Corporation and a part-time Senior Lecturer in the School of Geomatic Engineering, UNSW. He is Chairman of the IAG's Special Study Group 1.179 "Wide Area Modeling for Precise Satellite Positioning", and has authored over 100 journal and conference publications.

Chris Rizos, B.Surv. (UNSW) Ph.D. (UNSW) is professor and leader of the Satellite Navigation and Positioning (SNAP) Group at UNSW. He is Secretary of Section 1, "Positioning", of the IAG.

INTRODUCTION

Real-time kinematic GPS precise positioning has been playing an increasing role in both surveying and navigation, and has become an essential tool for precise relative positioning. However, reliable and correct ambiguity resolution depends on observations to a large number of GPS satellites. This constrains its performance, making it difficult to address positioning applications in areas where the number of visible satellites is limited. The most obvious way to increase the number of tracking satellites is to integrate the GPS and GLONASS systems. Due to the different signal frequencies for the different GLONASS satellites, the commonly used DD procedure for carrier phase data processing cannot be implemented in its simplest form, as is done with GPS. To overcome this problem several modelling methods have been proposed in the literature. Three general classes of integrated GPS and GLONASS functional models have been developed in the last decade. The first class is to introduce the known relative clock parameter, which is estimated using pseudo-range measurements, into the GLONASS DD carrier phase observation equations (Pratt et al., 1998; Leick, 1998). The second class is to estimate the clock parameters, baseline vectors and ambiguity parameters together in both the carrier phase and pseudo-range observation equations (Zhodzishsky, 1998; Kozlov, 1997; Wang, 1998; Han et al., 1999). However, for these two sets of techniques, the ambiguity resolution and positioning results are seriously affected by the remaining clock biases and the GLONASS pseudo-range inter-channel biases. The third method involves a two-level procedure or an iterative search approach to process DD observations (expressed in metres) without the receiver clock value (Wang, 2000; Habrich et al., 1999). For this third class of techniques, if the ambiguity sets can be fixed correctly, the positioning results are not affected by the clock bias. Unfortunately, in a two-level search approach any accepted wrong SD GLONASS ambiguity value at the GLONASS reference satellite can cause systematic model errors that may affect DD ambiguity resolution. The iterative search approach is only suitable for a long session static positioning. A detailed review of a variety of mathematical modelling options for integrated GPS and GLONASS can be found in Wang et al. (2001). In this paper three general classes of the integrated GPS and GLONASS functional models have been optimally integrated so that: (1) the ambiguity resolution is insensitive to the remaining clock biases and inter-channel biases, and (2) reliable and precise positioning results will not be affected by residual receiver clock biases.

High quality estimation results from the application of the Least Squares estimation technique requires specification of the optimal functional and associated stochastic model. The stochastic model is dependent on the choice of the functional model. Hence, for a different choice of functional model, the stochastic characteristics of unmodelled errors will be different, and the stochastic model must reflect this. Based on the

assumption that the accuracy of the one-way observations depends on signal-to-noise (Gianniou & Groten, 1996), or satellite elevation (Jin, 1995; Han, 1997), some approximate formulas to compute the variance-covariance matrix for DD observations have been proposed. However, constant coefficients for certain types of GPS receivers, which are empirically estimated from observations collected under specific observing conditions, are probably not well suited for other measurement environments. Due to the high temporal correlation of observations, the compensated method was proposed to estimate a scale factor in the stochastic model, using previous data collected over a certain period (Han, 1997). This method could derive a more realistic stochastic model, and hence increase the reliability of the ambiguity resolution and the positioning accuracy. However, it doesn't take into account the observations' spatial correlation, which would need refining of the of variance-covariance matrix. The construction of the variance-covariance matrix can be carried out using the residual series over the previous epochs, when the integer ambiguities are fixed correctly. Based on the estimated variance-covariance matrix of the residuals, and the relationship between the residuals and the observation errors, an improved variance-covariance matrix of the observations can be derived. Hence, the real-time stochastic model derived in this way will not only reflect the stochastic characteristics of the observation errors, but also the remaining biases due to multipath, atmospheric delay, inter-channel biases and orbital errors. This method could be used for different types (SD, DD, in metres or cycle units) of carrier-phase and pseudo-range observation combinations.

In this paper a novel data processing strategy for integrated GPS/GLONASS positioning, in combination with the real-time estimated stochastic model described above, is proposed. The performance of this data processing strategy will be demonstrated via examples of rapid static positioning and kinematic positioning.

FUNCTIONAL MODELING STRATEGY

The SD carrier phase observable between receivers can be expressed as (e.g. Leick, 1998):

$$I_1^p \mathbf{f}_{kl}^p = \mathbf{r}_{kl}^p + I_1^p N_{kl}^p - c \cdot dt_{kl} - I_{kl}^p / (f_1^p)^2 + T_{kl}^p + \mathbf{e}_{kl}^p \quad (1)$$

Where the subscripts k and l identify the ground receivers, and superscript p denotes the satellite. \mathbf{f}_{kl}^p is the SD carrier phase observable expressed in units of cycles. I_1^p and f_1^p are the wavelength and frequency of the L1 carrier wave. N_{kl}^p is the SD integer ambiguity; dt_{kl} is the difference between the two receiver clock biases in seconds; c is the speed of light; $I_{kl}^p / (f_1^p)^2$ is the SD ionospheric delay, where I is a function of the Total Electron Content; T_{kl}^p is the SD

tropospheric delay; and \mathbf{e}_{kl}^p is the carrier phase observation noise and remaining errors.

Equation (1) is valid for GPS and GLONASS carrier phase measurements. However, L1 GPS signals have the same frequencies for all satellites, while GLONASS signals have different frequencies for different satellites.

Double-Differenced Observables

The DD observable in units of metres can be formed as:

$$\begin{aligned} \mathbf{I}_1^p \mathbf{f}_{kl}^p - \mathbf{I}_1^q \mathbf{f}_{kl}^q &= \mathbf{r}_{kl}^{pq} + \mathbf{I}_1^p \cdot N_{kl}^p - \mathbf{I}_1^q \cdot N_{kl}^q + \\ &+ I_{kl}^p / (f_1^p)^2 - I_{kl}^q / (f_1^q)^2 + \mathbf{e}_{kl}^{pq} \end{aligned} \quad (2)$$

It could be seen that data processing for integrated GPS and GLONASS system becomes more complicated because of the different frequencies for the GLONASS satellites. The GLONASS DD observables have more ionospheric delay than the GPS DD observables. However it could still be ignored if the distance between the two receivers is short enough. Equation (2) could then be rewritten as:

$$\mathbf{I}_1^p \mathbf{f}_{kl}^p - \mathbf{I}_1^q \mathbf{f}_{kl}^q = \mathbf{r}_{kl}^{pq} + \mathbf{I}_1^p \cdot N_{kl}^{pq} - (\mathbf{I}_1^p - \mathbf{I}_1^q) \cdot N_{kl}^q + \mathbf{e}_{kl}^{pq} \quad (3)$$

It is clear that for GPS carrier phase measurements the third term on the right-hand side of Equation (3) will disappear. For GLONASS carrier phase measurements the third term, or the SD integer ambiguity for the reference satellite, must be estimated before the DD integer ambiguities can be computed. The remaining errors from the third term could cause systematic model errors and may result in wrong DD ambiguity resolution - and hence degraded positioning accuracy.

An alternative approach is to form the DD observable after the SD observables are expressed in units of cycles:

$$\begin{aligned} \mathbf{f}_{kl}^{pq} &= \left(\frac{f_1^p}{c} \mathbf{r}_{kl}^p - \frac{f_1^q}{c} \mathbf{r}_{kl}^q \right) - \left(\frac{I_{kl}^p}{c f_1^p} - \frac{I_{kl}^q}{c f_1^q} \right) \\ &+ \left(\frac{f_1^p}{c} T_{kl}^p - \frac{f_1^q}{c} T_{kl}^q \right) - (f_1^p - f_1^q) \cdot dt_{kl} + N_{kl}^{pq} + \mathbf{e}_{kl}^{pq} \end{aligned} \quad (4)$$

The differenced receiver clock bias cannot be eliminated in Equation (4). The second term (ionospheric delay) and the third term (tropospheric delay) will become slightly larger than in the case when the two frequencies are the same. Using GPS and GLONASS pseudo-range measurements, the difference between the two receiver clock biases can be estimated. It could be used to correct the second term for ambiguity resolution purposes. However, this receiver clock bias will significantly degrade the positioning accuracy.

An Integrated Three-Step Procedure

Due to the different frequencies for the different GLONASS satellites, the relative receiver clock bias Δdt cannot cancel in the GLONASS DD carrier phase (Equation (4)). To overcome this problem, the SD pseudo-range observations should be included. Although the pseudo-range-derived receiver clock is good enough for ambiguity resolution purposes, it still affects the positioning results. Therefore Equation (3) is used to determine the positioning results after the integer ambiguities are fixed. The third term on the right-hand side of Equation (3) will be considered an additional unknown parameter until a cycle slip occurs on the GLONASS reference satellite. Hence the data processing procedure can be summarised as follows.

Step 1: The DD GPS pseudo-range observables and the SD GLONASS pseudo-range observables are used:

$$\mathbf{P}_{kl,GPS}^{pq} = \mathbf{r}_{kl}^{pq} + \mathbf{e}_{kl}^{pq} \quad (5)$$

$$\mathbf{P}_{kl,GLONASS}^p = \mathbf{r}_{kl}^p + c \cdot dt_{kl} + \mathbf{e}_{kl}^p \quad (6)$$

Where $\mathbf{P}_{kl,GPS}^{pq}$ and $\mathbf{P}_{kl,GLONASS}^p$ are the DD GPS pseudo-range observable and the SD GLONASS pseudo-range observable respectively. Why are DD GPS pseudo-range observables used rather than SD GPS pseudo-ranges? When the difference of the two receiver clocks is introduced into the GPS SD observation equation, the inter-channel bias between the GPS satellite and the GLONASS satellite may be introduced in order to derive equivalent results, making the data processing more complicated. This model was also identified as an optimal functional model by Rapoport (1997).

In this step, the difference in the two receiver clock biases, the initial coordinates and their variance-covariance matrix, can be derived for the ambiguity resolution process in the next step.

Step 2: DD GPS and GLONASS carrier phase observables in units of cycles, e.g. Equation (4), will be used for ambiguity resolution. The second term on the right-hand side of Equation (4) will disappear for GPS measurements due to the fact that the same frequency is used for different GPS satellites. However, this term must be corrected using the difference of the two receiver clock biases.

The frequency difference between GLONASS signals is smaller than 12.9MHz for L1 observations, and less than 10.1MHz for L2 observations. Hence the difference in the two receiver clock biases can be expected to be less than 10ns (approximately 3 metres), and therefore this term can be corrected at the 0.1 cycle level. For ambiguity resolution purposes, the bias could be ignored without significant impact on the reliability. However, this error cannot be ignored when Equation

(4) is used to derive the positioning results. Furthermore, this term could not be considered as the same unknown parameter for different epochs.

Step 3: Although the integer ambiguity set could be determined in Step 2 using Equation (4), the positioning results will be affected by the receiver clock biases. However, the DD carrier phase observables in units of metres, eg. Equation (3), where the receiver clock biases are removed and the integer ambiguity set determined in Step 2, could be used. In this way the third term on the right-hand side of Equation (3) could be considered as an additional unknown parameter over different epochs until a cycle slip occurs on the GLONASS reference satellite.

This three-step procedure is an integrated way of processing combined GPS and GLONASS data, which takes advantage of features of the different DD combinations. It should be mentioned that: (1) the double-differencing operator is applied to the GPS measurements only or the GLONASS measurements only, rather than between GPS and GLONASS; and, (2) cycle slip detection at the GLONASS reference satellite is required, though not repair.

If a mixed double-differencing operator between GPS and GLONASS was used, the coefficient of the clock term will increase dramatically to a value between 26.6MHz and 39.5MHz for L1 observations, and from 18.4MHz to 28.5MHz for L2 observations. It is easily seen that the clock error effect on ambiguity resolution in the mixed formulation is more serious than in the separated formulation. The inter-channel bias must be accounted for in some way if the difference between GPS and GLONASS measurements is formed. Although inter-channel biases exist for measurements from different GLONASS satellites, they could be ignored for most applications. Hence the separated formulation of double-differences is much more reliable than the mixed formulation (Pratt et al., 1998). The slight disadvantage in the separated formulation is the reduced number of the double-differences (reduced by one). As with the case of the carrier phase, the performance of the separated pseudo-range combination is better than the mixed combination.

The second issue is cycle slip detection on the GLONASS reference satellite. It can be seen that the third term should be a constant when tracking at both receivers to the GLONASS satellite is maintained. However, when a cycle slip occurs on the SD carrier phase measurement involving the GLONASS reference satellite, this term will no longer be constant. A new unknown parameter must be introduced or this cycle slip must be repaired. One cycle slip will result in about 1.5mm for the L1 observations, and 2.0mm for the L2 observations, for the worst case. If the GLONASS reference satellite can be chosen from the middle of the GLONASS frequency range, it should be less than 1.0mm. Cycle slips should be detected by using the SD carrier phase observables (Equation (1)), which

contains a strong effect from the difference of the two receiver clock biases. In practice, only significant cycle slips were detected or were recorded by the receivers, and a new unknown parameter needed to be introduced.

REAL-TIME STOCHASTIC MODEL ESTIMATION

High quality results using Least Squares estimation techniques requires the correct selection of both the functional and stochastic models. The stochastic model is dependent on the choice of the functional model. Hence for a different choice of functional model, a different stochastic model may be needed. GPS and GLONASS observations are affected by several kinds of errors and biases. When forming the double-differences, the main biases are caused by multipath effects, residual atmospheric errors, orbital errors, and inter-channel biases. Due to insufficient knowledge about these physical phenomena, the above biases cannot be rigorously accounted for through functional modelling. The stochastic model has to therefore model both the observation noise and the unmodelled residual biases.

Empirical Stochastic Model

The well-known elevation dependent stochastic model is often used, which may be represented as an exponential function or an inverse of the sine of the satellite elevation angle (El-Rabbany, 1994; Jin, 1995). However, constant coefficients can only reflect error characteristics of the GPS receiver, rather than the unmodelled residual biases, which most probably are related to the observing environment. In order to introduce this "environment information", an adaptive stochastic model was proposed by Han (1997), in which a scale factor is introduced, and estimated in real-time:

$$\mathbf{S} = s \cdot (a_0 + a_1 \cdot \exp(-E/E_0)) \quad (7)$$

Where σ is the standard deviation of the carrier phase or pseudo-range observations; a_0 , a_1 and E_0 are approximated by constants; E is satellite elevation angle, and s is a scale factor, which can be estimated from moving 2-5 minute windows of data. This model more or less accounts for the environmental impact on the stochastic model. However, the spatial correlation between the DD observables cannot be refined in this way. In other words, the diagonal elements of the a priori variance-covariance matrix cannot be accounted for through the use of a scale factor, in place of the appropriate non-diagonal elements. Therefore the construction of more rigorous stochastic model is still a challenge. An adaptive Kalman filter has been investigated for real-time stochastic modelling for an integrated GPS/GLONASS/INS system (Wang, 1999).

Real-Time Stochastic Modeling

Based on the fact that the residual series of Least

Squares estimation contains sufficient information of the observation noise and biases, a more rigorous stochastic model is derived. The general Least Squares linearised observation equation and the criteria can be modelled as:

$$V_i = B_i X_i - L_i \quad (8)$$

$$V_i^T D_i^{-1} V_i = \text{Minimum} \quad (9)$$

Where V_i and L_i are the vectors of all the measurements and residuals at epoch i respectively; B_i is the design matrix related to the vector of measurements L_i ; X_i is the estimated unknown parameter matrix; and D_i is the variance-covariance matrix of the measurements.

Based on the minimum quadratic form of the residuals, the Least Squares estimated parameter \hat{X}_i are:

$$\hat{X}_i = (B_i^T D_i^{-1} B_i)^{-1} B_i^T D_i^{-1} L_i \quad (10)$$

Substituting Equation (10) into Equation (8), the estimated residuals are:

$$V_i = (B_i (B_i^T D_i^{-1} B_i)^{-1} B_i^T D_i^{-1} - E) L_i \quad (11)$$

The variance-covariance matrix can be derived from Equation (11):

$$D_i = Q_{V_i} + B_i (B_i^T D_i^{-1} B_i)^{-1} B_i^T \quad (12)$$

Where Q_{V_i} is the variance-covariance matrix of the residuals. Due to the similarity of the observation environments, the residuals of the observations show a high degree of temporal and spatial correlation in the short term. In other words, the residual series could be considered as a wide-sense stationary process. The actual variance-covariance matrix of the residuals can then be estimated from the previous residual series, whose ambiguity sets have already been fixed to the correct values, using the following equation:

$$Q_{V_i} = \frac{1}{N} \sum_{k=1}^N V_{i-k} V_{i-k}^T \quad (13)$$

Where N is the width of the moving window. The minimum N should not be less than the number of DD ambiguities. If N is too large, temporal and spatial decorrelation will occur, and the performance will decrease. Testing has shown that the optimal width of the moving window is in the range of 10-30 epochs with 1-second sampling rate. In practical applications, residuals from the ambiguities-fixed solutions need to be used because the float ambiguity values may absorb some unmodelled errors.

In Equation (12), the variance and covariance of the measurements cannot be estimated directly. An iterative procedure becomes necessary. The initial (or default) variance-covariance matrix is determined by using the previous variance-covariance matrix. Based on the previous measurement residuals, the variance-covariance matrix of the measurements can be rigorously estimated in real-time from Equations (12, 13). Normally iterating twice is enough. The default stochastic model should be used at the beginning of the data processing, or for a new satellite, or after a long data gap.

The stochastic model in this paper not only reflects the stochastic characteristics of the observation noise, but also the residual biases due to multipath, the atmospheric delays, the inter-channel biases and the orbital error remaining after double-differencing both the carrier phase and pseudo-range observations. With the help of the estimated variance-covariance matrix, the reliability of ambiguity resolution and the accuracy of the real-time kinematic positioning results can be significantly improved.

AMBIGUITY RESOLUTION, VALIDATION AND ADAPTATION

Equation (4) with the clock bias correction can be used to estimate the real-valued ambiguities and their variance-covariance matrix. The associated stochastic model is derived from the residual series over the previous epochs. The LAMBDA procedure is then implemented to search the integer ambiguity set (Teunissen, 1994; Han & Rizos, 1995). The validation criteria test suggested by Han (1997), and the ratio test, are implemented. If both tests are passed, the ambiguity resolution is assumed to be correct.

If the resolved integer ambiguities are incorrect, in general the wrong integer ambiguities will refer to more than one satellite pair, and it is almost impossible to identify which ambiguities are incorrect. However, the fact that some significant biases are present in the observations can be confirmed. If there are enough satellites, eg. more than 5 GPS satellites, or more than 5 GLONASS satellites, or more than 7 GPS and GLONASS satellites, some of these observations could be eliminated. Following the outlier detection algorithm based on correlation analysis theory (Shi, 1998; Dai et al., 1999), a procedure whereby one satellite is eliminated step-by-step has been implemented in the software (so that at least four DD carrier phase observables could still be formed). If ambiguity resolution has failed, the procedure is repeated until ambiguity resolution is successful, or less than four DD carrier phase observables can still be formed. If less than four DD carrier phase observables can be formed and the ambiguity test still fails, the ambiguity resolution procedure is considered to have failed. This adaptive procedure ensures that the ambiguity resolution success rate increases significantly (Han,

1997).

PERFORMANCE ANALYSIS OF A NOVEL DATA PROCESSING STRATEGY

In order to test the performance of the proposed data processing strategy, including the integrated three-step procedure to improve the functional model and the real-time stochastic modelling technique, the following rapid static positioning and kinematic positioning experiments were carried out.

Rapid Static Positioning Experiments

Rapid static positioning experiments were carried out over different distances using two GG24 integrated GPS/GLONASS single-frequency receivers. The reference receiver was set up on the Mather Pillar, on the roof of the Geography and Surveying building, at The University of New South Wales. The rover receiver was set up at different sites, which included the same roof nearby the reference receiver, at Coogee Beach, at Maroubra Beach, and at the La Perouse Beach. The baseline name, baseline length, number of satellites, observation span (total number of epochs) are given in Table 1. The positioning results can be easily checked from the repeatability of the baseline vectors for the different sessions. In all the data sets the cut-off elevation angle was set to 15 degrees during the processing.

Table 1. Details of the test data sets.

Name	Length (m)	GPS/GLONASS satellites	Total Epochs	Survey Date
A1	12	8-5/7-3	14362	12.5.99
A2	2873	9-5/7-4	4012	11.5.99
A3	4053	9-6/5-3	6868	10.5.99
A4	6796	7-5/4-3	4690	10.5.99

The observations were divided into different sessions, 10 seconds in length for one set of sessions and 1 minute in length for another set of sessions. The data processing results are listed in Table 2 for the 10-second sessions and in Table 3 for the 1-minute sessions. It can be seen that rapid static positioning derives solutions with more than 98.3% success rate using 10 seconds of data, and with 100% success rate using 1 minute of data for each session.

Table 2. Rapid static positioning results using 10 seconds of data for each session.

Name	Total sessions	Correct (%)	Reject (%)	Wrong (%)
A1	1406	1396(99.3%)	10(0.7%)	0(0.0%)
A2	401	401(100.0%)	0(0.0%)	0(0.0%)
A3	631	629(99.7%)	2(0.3%)	0(0.0%)
A4	418	411(98.3%)	7(1.7%)	0(0.0%)

Table 3. Rapid static positioning results using 1 minute of data for each session.

Name	Total sessions	Correct (%)	Reject (%)	Wrong (%)
A1	233	233(100.0%)	0(0.0%)	0(0.0%)
A2	66	66(100.0%)	0(0.0%)	0(0.0%)
A3	109	109(100.0%)	0(0.0%)	0(0.0%)
A4	75	75(100.0%)	0(0.0%)	0(0.0%)

The rapid static positioning results (1 minute for each session, Baseline A2) were also derived using Equation (4), in which the clock biases are considered unknown parameters, and plotted in Figure 1 (gray colour, relative to the GPS-only solution using the whole data set). Comparing against the positioning results (black colour, relative to the GPS-only solution using the whole data set) derived using Equation (3), in which the third term of the SD integer ambiguity for the reference satellite is considered an unknown parameter, it is clear that the suggested procedure derives positioning solutions with higher accuracy.

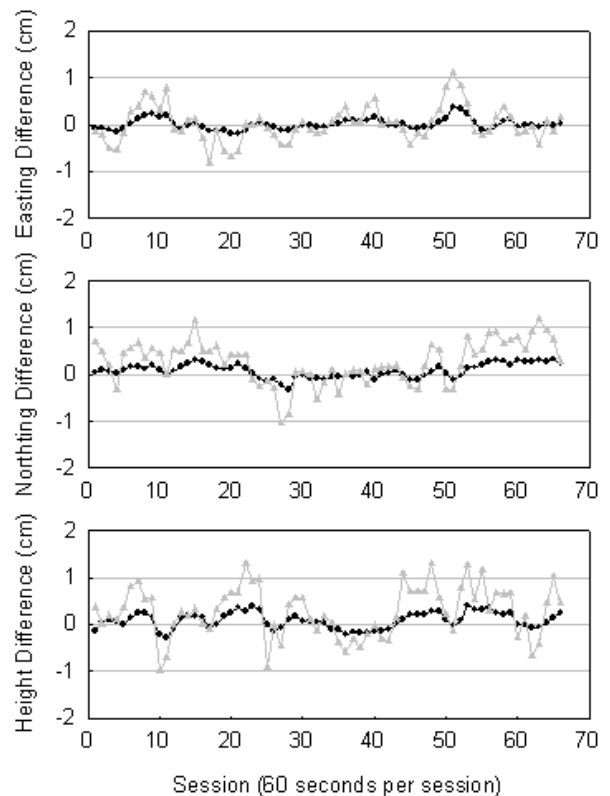


Figure 1. Rapid static positioning results for 1 minute sessions using Equations (3) (gray) and (4) (black) for Baseline A2.

Kinematic Positioning Experiments

All static baselines were processed in the kinematic positioning mode in order to test the performance of the proposed procedure using a single epoch of data. In this mode, at least 3 GPS satellites, 3 GLONASS satellites,

and total of 8 GPS and GLONASS satellites are required for data processing.

Data processing has been carried out for the static data using two different stochastic models. One is the empirical stochastic model dependent on the satellite elevation angle, and the other one is the real-time stochastic model estimated using the residual series from previous epochs proposed in this paper. The results are listed in columns 3-5 in Table 4 and Table 5. The third column is the number (and percentage) of epochs for which ambiguity resolution is successful on an epoch-by-epoch basis. The fourth column is the number of epochs (and percentage) which do not pass the validation criteria test. The fifth column is the number of epochs (and percentage) which pass the validation criteria tests, but for which the result is incorrect. It can be seen that using the elevation-dependent empirical stochastic model the success rates for single-epoch ambiguity resolution range from 80.1% to 83.3%. It also shows that quite a large percentage of epochs (0.2%) at Baseline A1 give the wrong ambiguity resolution results. If the real-time stochastic model estimated using the residuals from the previous epochs (e.g. 10 epochs) were used, the success rates of ambiguity resolution range from 95.9% to 99.98%, and no wrong ambiguity resolution results are accepted. The results indicate that single-epoch ambiguity resolution can achieve very high success rates with redundant GPS and GLONASS satellite observations. The conclusion that can be drawn is that the estimated stochastic model from the residuals is in theory more rigorous, and in practice more powerful, than using other forms of arbitrary stochastic modelling.

Table 4. Single-epoch solution using the elevation-dependent empirical stochastic model.

Name	Total Epochs	Correct (%)	Reject (%)	Wrong (%)
A1	14361	11689(81.4%)	2639(18.4%)	33(0.2%)
A2	4012	3335(83.1%)	677(16.9%)	0(0.0%)
A3	6868	5723(83.3%)	1145(16.7%)	0(0.0%)
A4	4690	3759(80.1%)	931(19.9%)	0(0.0%)

Table 5. Single-epoch solution using the real-time stochastic model derived using residuals from previous epochs, as proposed in this paper.

Name	Total Epochs	Correct (%)	Reject (%)	Wrong (%)
A1	14361	14015(97.60%)	346(2.40%)	0(0.0%)
A2	4012	4011(99.98%)	1(0.02%)	0(0.0%)
A3	6868	6589(95.9%)	279(4.1%)	0(0.0%)
A4	4690	4845(96.1%)	182(3.9%)	0(0.0%)

The ratio values for the validation criteria are plotted at

each epoch in Figure 2 for Baseline A2. The grey and black dots in Figure 2 are ratio values from the elevation-dependent empirical stochastic model and the estimated stochastic model from residuals, respectively. It can be seen that the ratio values using the estimated stochastic model from residuals are much bigger than those using the elevation-dependent empirical stochastic model. It is believed that the larger the ratio values the more reliable the ambiguity resolution.

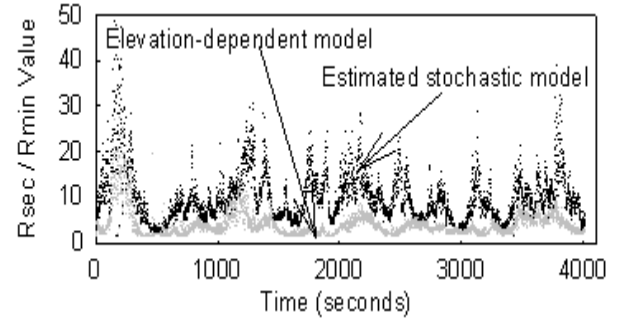


Figure 2. Ratio values for different stochastic models.

The positioning results are also derived using two different stochastic models for Baseline A2. The differences of the three coordinate components, between the single-epoch solutions and the final baseline solution using whole data set, are plotted in Figure 3. The gray and black curves are positioning results using the elevation-dependent empirical stochastic model (gray) and the estimated stochastic model from residuals (black), respectively. It can be seen that a realistic stochastic model can significantly improve the accuracy of the final positioning solutions.

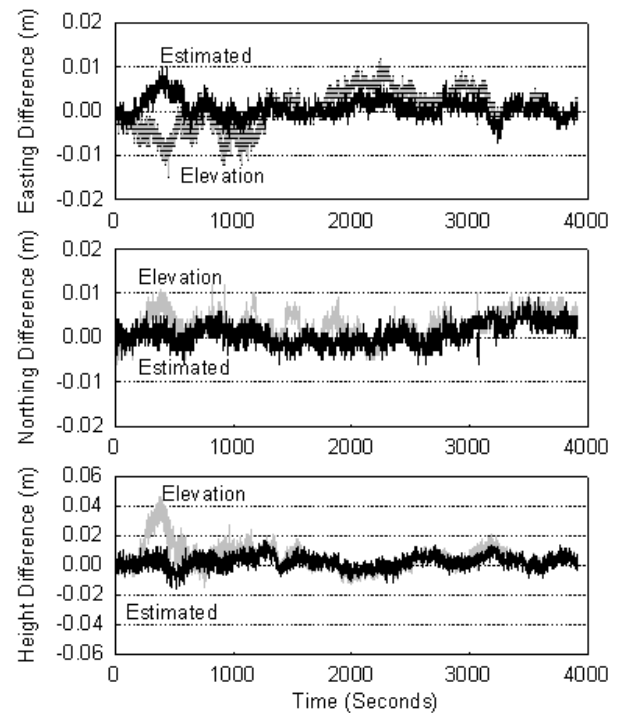


Figure 3. Positioning results using the elevation-dependent empirical stochastic model (gray) and the estimated stochastic model from residuals (black).

A further kinematic experiment was carried out on 29 April 1999 using two GG24 GPS/GLONASS single-frequency receivers and three dual-frequency Leica SR399 GPS receivers. One GG24 receiver and one Leica SR399 were set up at the reference site. The other GG24 receiver and the two Leica GPS receivers were mounted on a car. The trajectory of the rover receivers is shown in Figure 4. (The purpose of using two Leica dual-frequency receivers is as a check on the derived GG24 positioning results.) The experiment started at the side of the M4 Motorway, Sydney, which is nearby the reference site. After the first 40 minutes in static mode, the car moved along the Motorway and the Great Western Highway, finishing the experiment in static mode again for 15 minutes. This concludes a single loop. A total of two loops were completed with 1Hz data rate, and a total of 7571 epochs of data were collected. The number of observed satellites is plotted in Figure 5.

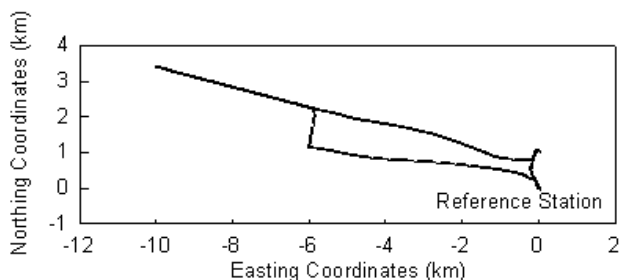


Figure 4. Trajectory of the rover receivers relative to the reference site.

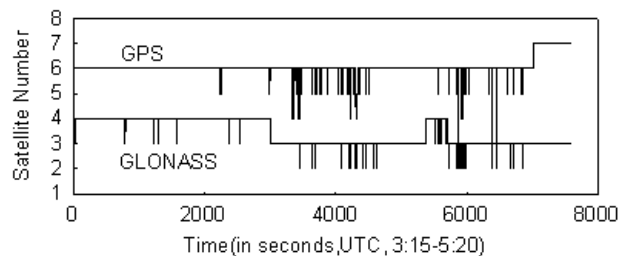


Figure 5. Number of observed satellites.

In this kinematic experiment data was divided into two groups according to the baseline length. The baseline lengths in one group were those less than 6km. The baseline lengths in the second group range from 6km to 11km. The results are summarised in Table 6. In order to check the kinematic results the Leica GPS receivers were used, as correct and reliable results from dual-frequency GPS receivers can be achieved using current ambiguity resolution techniques. If the distance differences between the Leica rover receivers and the GG24 rover receiver exceeded some defined tolerance value (5cm in this experiment), the ambiguities for the GG24 receivers were considered to have been fixed to the wrong values. From Table 6 it can be seen that using the elevation-dependent empirical stochastic model the success rate for ambiguity resolution is only 72.9% with the first short-range group, and a very poor 19.2% for distances ranging from 6-11km. The percentage of rejected epochs is 27.1% and 80.8%,

respectively. If the real-time stochastic model estimated using the residual series from the previous epochs is used, the success rate for ambiguity resolution is significantly improved to 94.6% for the short-range group and 56.4% for distances ranging from 6 to 11km. It can be seen that for the short-range baselines, the positioning results can achieve a reasonable success rate. However, when the distance between the two receivers is longer than about 6km, the success rate decreases quickly using single-frequency GG24 GPS/GLONASS receivers, if only a single epoch of data are used.

Table 6. GG24 kinematic positioning results Using a single epoch of data.

Total Epochs	Dist. (km)	Correct (%)	Reject (%)	Wrong (%)
Elevation dependent empirical model				
6331	<6	4616 (72.9%)	1715 (27.1%)	0 (0.0%)
1240	6-11	238 (19.2%)	1002 (80.8%)	0 (0.0%)
Estimated stochastic model				
6331	<6	5988 (94.6%)	343 (5.4%)	0 (0.0%)
1240	6-11	699 (56.4%)	541 (43.6%)	0 (0.0%)

CONCLUDING REMARKS

A new data processing strategy for integrated GPS/GLONASS positioning using a three-step procedure, and associated real-time stochastic model estimated using residuals from the previous epochs, has been introduced in this paper. The proposed functional model improves the performance because the ambiguity resolution process is insensitive to the residual clock biases and the inter-channel biases, and hence reliable and precise positioning results are obtained. The real-time stochastic model estimated from the residuals can significantly improve the ambiguity resolution success rates, as well as the accuracy of the final solutions.

The results indicate that rapid static positioning requires 10 seconds of data for success rates over 98%, or just 1 minute of data for a success rate of 100%, based on four experiments carried out over distances less than 6km. The single-epoch solution for kinematic positioning could achieve a 94.6% success rate over distances shorter than 6km. However, when the range increases the success rate dramatically decreases. Investigations are underway concerning the optimal strategy for dual-frequency GPS/GLONASS processing.

ACKNOWLEDGEMENTS

The first author is supported by an International Postgraduate Research Scholarship (IPRS).

REFERENCES

- Dai, L., S. Han & C. Rizos (1999). A multiple outlier detection algorithm for instantaneous ambiguity resolution for carrier phase-based GNSS positioning. *Int. Symp. on Digital Earth (ISDE)*, Beijing, P.R. China, 29 November - 2 December, 321-332.
- El-Rabbany, A.E-S. (1994). The effect of physical correlations on the ambiguity resolution and accuracy estimation in GPS differential positioning. Ph.D. Dissertation, Dept. of Geodesy & Geomatics Eng., Tech. Rept. No.170, University of New Brunswick, Canada, 161pp.
- Gianniou, M. & E. Groten (1996). An advanced real-time algorithm for code and phase DGPS. *Proc. 5th Int. Conf. on Differential Satellite Navigation Systems*, St. Petersburg, Russia, 20-24 May.
- Habrigh, H., G. Beutler, W. Gurtner & M. Rothacher (1999). Double difference ambiguity resolution for GLONASS/GPS carrier phase. *12th Int. Tech. Meeting of the Satellite Division of the U.S. Inst. of Navigation*, Nashville, Tennessee, 14-17 September, 1609-1618.
- Han, S. (1997). Quality control issues relating to ambiguity resolution for real-time GPS kinematic positioning. *Journal of Geodesy*, 71(6),:351-361.
- Han, S. & C. Rizos (1995). A new method for constructing multi-satellite ambiguity combinations for improved ambiguity resolution. *8th Int. Tech. Meeting of the Satellite Division of the U.S. Inst. of Navigation*, Palm Springs, California, 12-15 September, 1145-1153.
- Han, S., L. Dai & C. Rizos (1999). A new data processing strategy for combined GPS/Glonass carrier phase-based positioning. *12th Int. Tech. Meeting of the Satellite Division of the U.S. Inst. of Navigation*, Nashville, Tennessee, 14-17 September, 1619-1627.
- Jin, X.X. (1995). The change of GPS code accuracy with satellite elevation. *Proc. 4th Int. Conf. on Differential Satellite Navigation Systems*, Bergen, Norway, 24-28 April.
- Kozlov, D. (1997). Instant RTK cm with low cost GPS+GLONASS™ C/A receivers. *10th Int. Tech. Meeting of the Satellite Division of the U.S. Inst. of Navigation*, Kansas City, Missouri, 16-19 September, 1559-1569.
- Leick, A. (1998). GLONASS satellite surveying, *Journal of Surv. Eng.*, 121, 91-99.
- Pratt, M., B. Burke & P. Misra (1998). Single-epoch integer ambiguity resolution with GPS-GLONASS L1-L2 data. *11th Int. Tech. Meeting of the Satellite Division of the U.S. Inst. of Navigation*, Nashville, Tennessee, 15-18 September, 389-398.
- Rapoport L. (1997). General purpose kinematic/static GPS/GLONASS postprocessing engine. *10th Int. Tech. Meeting of the Satellite Division of the U.S. Inst. of Navigation*, , 16-19 September, 1757-1772.
- Teunissen, P.J.G. (1994). A new method for fast carrier phase ambiguity estimation. *IEEE Position Location & Navigation Symposium PLANS94*, Las Vegas, Nevada, 11-15 April, 562-573.
- Wang, J. (1998). Mathematical models for combined GPS and GLONASS positioning. *11th Int. Tech. Meeting of the Satellite Division of the U.S. Inst. of Navigation*, Nashville, Tennessee, 15-18 September, 1333-1344.
- Wang, J. (1999). Stochastic modelling for RTK GPS/GLONASS positioning. *Navigation*, 46(4), 297-305.
- Wang, J. (2000). An approach to GLONASS ambiguity resolution. *Journal of Geodesy*, 74(5), 421-430.
- Wang, J., C. Rizos & M.P. Stewart (2001). GPS and GLONASS integration: Modelling and ambiguity resolution issues. *To be published in GPS Solutions*.
- Shi, C. (1998). Large scale GPS network adjustment & analysis theory and its application. Ph.D. Dissertation, The School of Geoscience and Engineering Surveying, Wuhan Technical University of Surveying and Mapping, pp.123 (in Chinese).
- Zhodzishsky, M., M. Vorobiev, A. Khvalkov & J. Ashjaee (1998). Real-Time Kinematic (RTK) processing for dual-frequency GPS/GLONASS. *11th Int. Tech. Meeting of the Satellite Division of the U.S. Inst. of Navigation*, Nashville, Tennessee, 15-18 September, 1325-1331.